

IMAGING E-SELECTIN EXPRESSION FOLLOWING TRAUMATIC BRAIN INJURY IN THE RAT USING A TARGETED USPIO CONTRAST AGENT.

Catherine Chapon¹, Florence Franconi², Franck Lacoeyille¹, François Hindré¹, Patrick Saulnier¹, Jean-Pierre Benoit¹, Jean-Jacques Le Jeune¹ and Laurent Lemaire¹

Short title: E-selectin mapping in brain traumas

¹ INSERM, U 646, Ingénierie de la Vectorisation, Angers, F-49100 France ; Université d'Angers, UMR-S646, Angers, F 49100 France.

² Service Commun d'Analyses Spectroscopiques, Université of Angers, France.

Correspondance to:

Dr Laurent LEMAIRE

INSERM U 646

“Ingénierie de la Vectorisation Particulaires”

10, rue André Boquel

49100 Angers, France.

Tel.: +33 241 735855

Fax.: +33 241 735853

Abstract:

The aim of this work was to map E-selectin expression in a traumatic brain injury model using a newly-designed MR contrast agent. Iron cores, responsible for susceptibility effects and therefore used as T2* contrast agents, need to be coated in order to be stabilized and need to be targeted to be useful. We have designed a molecule coating composed, at one end, of bisphosphonate to ensure anchorage of the coating on the iron core and, at the other end, of Fukuda's defined heptapeptide known to target selectin binding sites. The synthesized nanoparticles were able to non-invasively target the traumatic brain lesion, inducing a specific T2* decrease of about 25% up to at least 70 minutes post-injection of the targeted contrast agent.

Keywords:

Brain - trauma - selectin - MRI – SPIO.

Abbreviations:

IL1- β and TNF- α : Interleukin-1- β and tumor necrosis factor- α

IELLQAR: Isoleucine-glutamate-leucine-leucine-glutamine-alanine-arginine heptapeptide

BP: bisphosphonate

^{99m}Tc -BP: Technetium chelated to bisphosphonate

EG3: Ethylene glycol block repeated 3 times.

Hd: Hydrodynamic diameter.

ζ : zeta potential.

e: polyelectrolyte accessible layer depth

d_q : charge density (in C/m^3)

RARE: Rapid Acquisition with Relaxation Enhancement

ADC: Apparent Diffusion Coefficient

3DmGE : 3D multi-Gradient Echos sequence

Introduction:

Traumatic brain injury is a worldwide problem that results in death and disability for millions of people every year. Currently, in developed countries, it is estimated that traumatic brain injury is responsible for 1.5–2‰ of deaths and that 2-3‰ of the population lives with permanent disabilities[1-3]. The most common and serious consequence of traumatic brain injury is brain edema, or more precisely, brain edemas. Indeed, on one hand, one can depict a cytotoxic edema that results from an osmotically-driven shift of water from the extracellular space into the cell [4] as a consequence of cellular sodium influx and potassium efflux [5, 6] and on the other hand, a vasogenic edema occurring with the extravasation of fluid into the extracellular space following transient blood–brain barrier permeation that may also promote or aggravate cell swelling. Associated to these water shifts, recent brain injury studies have indicated that resident brain cells are capable of synthesizing a wide variety of cytokines and chemokines as well as promoting the expression of intercellular adhesion molecules that attract peripheral inflammatory leukocytes to the site of injury [7-10] and may contribute to the injury process [7, 11]. Among the intercellular adhesion molecules, E-Selectin (CD62E and ELAM-1), a C-type lectin of 97 kDa, is involved in the leukocyte rolling and recruitment phases [12-15] and could then be a potential pharmacological target [16]. Although mapping of selectin expression *in vivo* has been performed using MR imaging [4, 17-23], SPECT imaging [24, 25], optical imaging [21, 26] and ultrasound imaging [27-29] in well-established inflammatory models after injection of pro-inflammatory molecules (IL-1 β or TNF- α) [18, 27], or oxazolone [22], selectin mapping in brain traumas has not yet been explored. Currently, targeting properties can be given to the imaging probes via three types of molecules linked to those probes. Thus, either the well-known carbohydrate antigen or its synthetic mimetic molecule, Sialyl LewisX (sLeX) [18-20, 30], or an anti E-selectin

monoclonal antibody F(ab')₂ [17, 21, 22, 24-27] or short amino-acid chains [21, 25] are grafted.

For all these imaging techniques and targeting opportunities, the present research focuses on 1) the design of a new USPIO, coated with a short heptapeptide, as defined by Fukuda [31], and 2) the mapping of E-selectin expression *in vivo* with a high resolution as accessible with MRI in a traumatic brain injury model.

Methods

Fluid percussion–induced brain injury

Animal care was carried out in compliance with the relevant European Community regulations (*Official Journal of European Community* L358 12/18/1986). Female Sprague-Dawley rats (230–270 g) were supplied by Angers University Hospital animal facility; they were anaesthetized with isoflurane via a stereotactic-compatible nose cone (Minerve, Esternay, France), being induced at 5% and maintained at 1.5% throughout the entire procedure. Once induced, the animal was placed in a stereotactic frame. A scalp incision was made, the scalp and temporal muscles were reflected, and a 2.5mm-diameter craniotomy was carried out above the left auditory cortex, 2mm posterior to the lateral suture. A fitting tube, connected to the fluid lateral percussion device, was cemented into the open craniotomy site. A 20-msec pulse at a pressure of 2.0 ± 0.1 atm induced fluid lateral-percussion brain injury. Immediately after fluid lateral percussion, the scalp incision was sutured and the rats were allowed to recover from anaesthesia. Normothermia was maintained at 36.5–37.5°C by using a heating pad placed under the animal during all surgical procedures and in the acute, post-injury period. Thereafter, the rats were housed in temperature- and light controlled conditions,

with food and water *ad libitum*. Sham-operated rats underwent the same surgery except for percussion.

Synthesis of a radiolabeled peptide

IELLQAR was proven to efficiently inhibit the binding of sialyl Lewis X or sialyl Lewis A oligosaccharides to E-selectin [31] or leukocyte infiltration in heart transplants [32] and therefore may be a relevant heptapeptide for E-selectin targeting. Thus, this peptide was grafted on an aminobisphosphonate (Surfactis Technologies, Angers, France) capable of chelating ^{99m}Tc . The synthesized molecule was then called BP-IELLQAR (MW: 1,345g.mol⁻¹). Radiolabeling was performed by incubating 27mCi ^{99m}Tc with 3μmole of BP-IELLQAR.

Radiochemical purity of the radiolabeled peptide

The radiochemical purity was measured by thin-layer chromatography (TLC). The method used a 10*2.5cm² strip of silica gel impregnated glass fiber sheet, ITLCTM SG, (Pall corporation, Saint Germain en Laye, France) as the solid phase and dimethyl ketone as the mobile phase. 2 μL of ^{99m}Tc -BP-IELLQAR were spotted on the strip and eluted. The strip was then imaged using a Cyclone Storage Phosphor Scanner (Perkin Elmer, Courtaboeuf, France). Using TLC assay, radiolabeled ^{99m}Tc -BP-IELLQAR is not eluted by the mobile phase whereas free ^{99m}Tc moves in the dimethyl ketone solvent front. Radiochemical purity was calculated as the ratio of activity at the origin (^{99m}Tc -BP-IELLQAR) to the whole activity of the strip (^{99m}Tc -BP-IELLQAR + ^{99m}Tc).

Gamma-counting protocol

Sham-operated rats (n =6) and traumatized rats were injected via the tail vein with ^{99m}Tc -BP-IELLQAR (1.3mCi), 1h (n=6), 24 h (n=3) or 72h (n=3) post-trauma. The animals were

sacrificed under deep anaesthesia 1h post-injection and their brains were sliced in 2mm sections for gamma-counting. Activity was normalized to sample weights.

Synthesis of the targeted and non-targeted MR contrast agents

Iron oxide can be used as an MR contrast agent. However, in order to be stable in physiological conditions, the iron core, obtained by co-precipitation of an aqueous solution of $\text{Fe}^{2+}/\text{Fe}^{3+}$ iron salts in a tetramethylammonium hydroxide solution [33], has to be coated. Numerous coatings have been developed among which are molecules carrying bisphosphonate groups [34, 35]. Therefore, the stabilisation of the iron cores was performed with either 100% BP-EG3, BP-EG3 (MW = 342g.mol⁻¹) being a bisphosphonate on which 3 ethyleneglycol blocks were grafted (Surfactis Technologies, Angers, France) for the non-targeting coating or a mixture of BP-IELLQAR/ BP-EG3 (10%/90% mol/mol) for the targeted nanoparticulate contrast agent.

Size, zeta potential, charge density, polyelectrolyte accessible layer, R2 relaxivity and iron load of the targeted and non-targeted MR contrast agents

The nano-emulsion characterization, hydrodynamic diameter (Hd in nm), zeta potential (ζ in mV), polyelectrolyte accessible layer depth (e in nm) and its related charge density (d_q in C/m³) measurements were carried out by dynamic light scattering using a Nano ZS apparatus, Malvern Instruments (Orsay, France). The Helium-Neon laser, 4 mW, operates at 633 nm, with the scatter angle fixed at 173°, and the temperature at 25 °C. d_q and e were obtained by measuring the electrophoretic mobility of the nanoparticles at varying NaCl concentrations and after fitting to the so called 'soft particles analysis' model [36, 37]. R2 relaxivities were defined at 7T on a Bruker DRX300 (Bruker, Wiessembourg, France) using a CPMG

sequence. The iron load was determined by a spectrophotometric method after acidic digestion of the iron core as previously described [33].

Magnetic Resonance Imaging protocol

Experiments were performed with a Bruker Avance DRX 300 (Bruker, Wiessembourg, France) equipped with a vertical superwide-bore magnet and shielded gradient insert. The resonant circuit of the NMR probe was a 38-mm-diameter birdcage. Body temperature was maintained at 36.5–37.5°C by using a feedback-regulated heating pad. A 3-mm-thick diffusion-weighted image was taken, located at the centre of the lesion. In order to reach an acceptable signal-to-noise ratio without dramatically increasing the acquisition time, a 96 * 96 matrix for FOV = 3 * 3cm was used, leading to an in-plane resolution of 312 µm. Diffusion-weighted images were obtained using a Stejskal-Tanner-type pulsed gradient stimulated echo sequence [38] with three diffusion weighting factor values (b)= 95, 503 and 1,303 sec/mm² [$b = (\gamma G \delta)^2 (\Delta - \delta/3)$], where γ = gyromagnetic ratio; gradient strength $G = 100\text{mT/s}$; gradient duration $\delta = 5\text{msec}$; duration between the leading edges $\Delta = 100\text{ms}$. The diffusion-sensitizing gradient was placed only along the direction of the slice selection gradient (i.e., rostro-caudally) regardless of the usual practice of calculating the Apparent Diffusion Coefficient (ADC) from a set of at least three orthogonal directions in order to reduce potential pitfalls due to brain anisotropy. We based our decision to carry out ADC calculations on a single direction on Van Putten's results in a Traumatic Brain injury model showing no anisotropy [39], and on Lythogoe's results showing that, in rat parietal cortex [40], the trace value calculated from the three orthogonal sets was close to the value measured with the diffusion gradient positioned rostrocaudally. In order to improve image quality, ECG synchronisation

was performed (Rapid Biomed, Wurzburg, Germany) and two averages were recorded. The minimal TR was set to 1,500msec whereas TE and mixing time (TM) were set at TE/TM = 22.7/88.1msec. The imaging time was then limited to about 10 minutes.

3D multi-Gradient Echo (3DmGE) imaging[41] was performed prior to and after BP-IELLQAR coated nanoparticles (n=5) or BP-EG3 coated nanoparticles (n=5) injection via the tail vein. Acquisitions were performed prior to and for 70 min after injection with the following parameters: FOV 30*30*15mm³, matrix 128*128*32, TR= 110ms, 6 TEs, TE₁ = 3ms, InterEchoTime = 3.14ms. The total acquisition time was then set to 8minutes.

ADC and T2* maps were calculated by mono-exponential fitting of the experimental points using Bruker Paravision 4.0® software. Reported values for ADC and T2* were measured from manually drawn ROIs (15-30 pixels) defined on the diffusion maps before being pasted on each data set. With respect to the spreading of T2* values from one individual to another, each lesion was defined as its own control and the initial T2* values were then set to 100%.

Rats were injected 2h post trauma, via the tail vein with either the non-targeted MR contrast agent (n = 5) or with the targeted MR contrast agent (n = 5).

Statistical Analysis

Data are expressed as mean ± SEM. Statistical analysis was performed using a bi-factorial analysis of variance (ANOVA) with a multiple-least-square analysis.

Results

Radiochemical purity of the radiolabeled probe; Fixing the probe

TLC analysis revealed that > 99% of the ^{99m}Tc radioactivity was peptide-bound. Tail vein injection of ^{99m}Tc BP-IELLQAR in sham-operated rats induced a left brain activity of 152 ±

21cpm/mg fresh tissue 1h post-injection. At the same time, activity in the right brain was measured at 154 ± 16 cpm/mg fresh tissue.

Brain counts in traumatized animals are presented in **Figure 1**. Briefly, brain activity in the ipsilateral hemisphere of rats experiencing traumatic brain injury always increases compared to the contralateral hemisphere ($p = 0.041$). Therefore, when injections were performed 1h, 24h or 72 h post trauma, 220 ± 69 , 240 ± 14 and 365 ± 150 cpm/mg of fresh tissue was measured in the left hemisphere which had experienced the trauma, compared to 122 ± 35 , 182 ± 36 and 132 ± 14 cpm/mg of fresh tissue in the contralateral hemisphere.

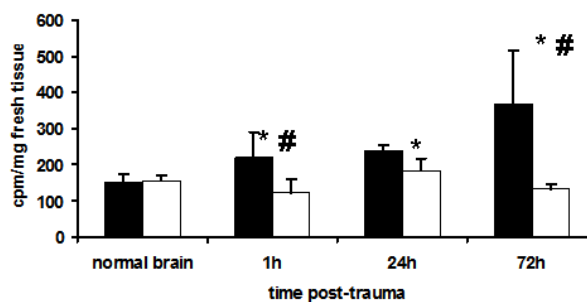


Figure 1: Comparison of selectin expression in sham and traumatized rat brains as a function of time using γ -counting after injection of ^{99m}Tc BP-IELLQAR.

* $p < 0.05$ compared to untraumatized brains.

$p < 0.05$ compared to contralateral brain at the same time point. The black boxes correspond to the traumatized hemisphere, the white boxes to contralateral hemisphere.

Physical properties of the MR contrast agents

BP-IELLQAR coated MR contrast agent had a hydrodynamic diameter $H_d = 25.3 \pm 1.3\text{nm}$, a zeta potential $\zeta = -34.1 \pm 0.3\text{mV}$, a charge density $d_q = -6.4 \cdot 10^6\text{C/m}^3$, a polyelectrolyte accessible layer (e) = 1nm, a longitudinal relaxivity $R_2 = 149 \pm 9\text{mmol}^{-1}\cdot\text{s}^{-1}\cdot\text{L}$ and an iron load of $1.4 \pm 0.1\text{mg/ml}$. The coating of the iron core with BP-EG3 led to nanoparticles whose $H_d = 16.7 \pm 0.1\text{nm}$, $\zeta = -26.8 \pm 1.0\text{mV}$, $d_q = -6.4 \cdot 10^6\text{C/m}^3$, $e = 1\text{nm}$, $R_2 = 150 \pm 17\text{mmol}^{-1}\cdot\text{s}^{-1}\cdot\text{L}$ and an iron load of $1.2 \pm 0.3\text{mg/ml}$.

MR imaging with non-targeted MR contrast agent

Rat brain traumas were confirmed by a standard diffusion-weighted imaging sequence and were limited to the cortex (**Figure 2a**). Brain lesions were characterised by a significantly reduced apparent diffusion coefficient $\text{ADC}_{\text{lesion}} = 0.38 \pm 0.02 \cdot 10^3 \text{mm}^2\cdot\text{sec}^{-1}$ ($n = 5$) compared to the contralateral cortex, $\text{ADC}_{\text{cortex}} = 0.71 \pm 0.05 \cdot 10^3 \text{mm}^2\cdot\text{sec}^{-1}$ ($n = 5$), ($p < 0,001$). Prior to MR contrast agent injection, 3DmGE were acquired (**Figure 2c**) and allowed the calculation of T_2^* values in the entire brain and specifically in the area of reduced ADC where a value of $T_2^*_{\text{lesion}} = 30.9 \pm 3.0 \text{ms}$ ($n = 5$) was measured, value significantly reduced compared to the contralateral cortex, $T_2^*_{\text{cortex}} = 39.4 \pm 3.3 \text{ms}$ ($n = 5$), ($p < 0.02$). However, with respect to the spreading of T_2^* values from one individual to another, each lesion was defined as its own control and the initial T_2^* values was then set to 100%. T_2^* evolution with time after the injection of BP-EG3-coated nanoparticles is shown in **Figure 3a**. At the first time point, post BP-EG3 coated nanoparticles injection, a significant 30% reduction in T_2^* values, both in the lesion ($p = 0.0024$) and the contralateral cortex ($p = 0.0005$) was observed. The signal smoothly recovered the pre-injection value after an additional 30 minutes, both in the non-traumatized and traumatized cortices (**Table 1**).

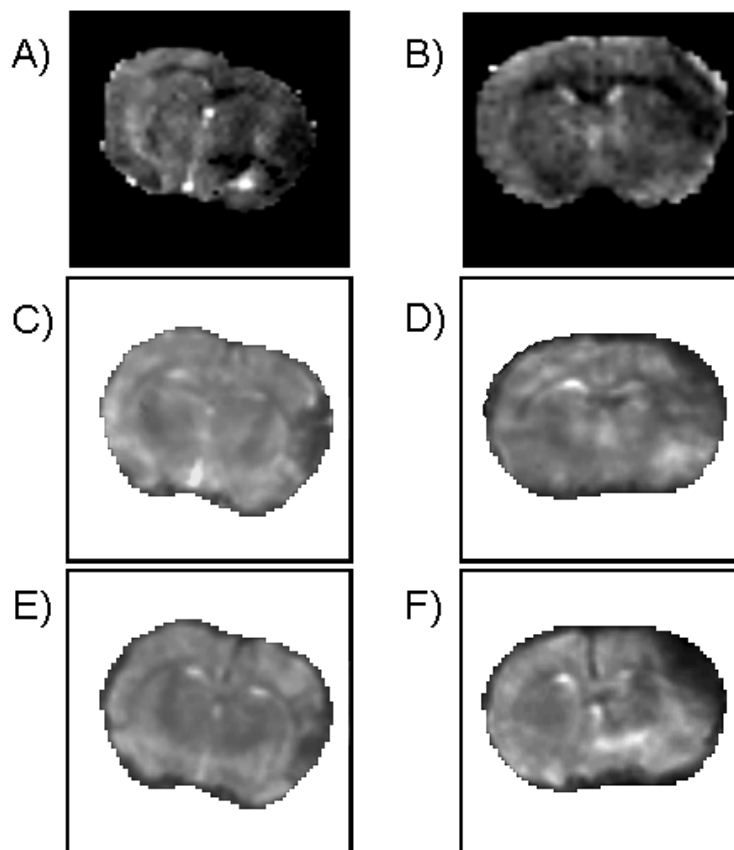


Figure 2: Typical ADC maps of rat brains about 1h after traumatic brain injury (A & B). Frame C presents the T2* map corresponding to frame A prior to BP-EG3 (non-targeted nanoparticles) and frame E 70 min after injection. Frame D presents the T2* maps corresponding to frame B prior to BP-IELLQAR (targeted nanoparticles) and frame F, 70 min after injection.

MR imaging with targeted MR contrast agent

Standard diffusion-weighted imaging sequence was also used to depict the traumatized brain and showed that the lesions were limited to the cortex in this second group of rats (**Figure 2b**). ADC in the lesioned cortex was measured at $ADC_{\text{lesion}} = 0.35 \pm 0.05 * 10^3 \text{ mm}^2.\text{sec}^{-1}$ (n = 5), a significantly reduced level compared to the contralateral cortex where a value of $ADC_{\text{cortex}} = 0.65 \pm 0.02 * 10^3 \text{ mm}^2.\text{sec}^{-1}$ (n = 5) was measured (p < 0.001). 3DmGE images acquired prior to MR contrast agent injection (**figure 2d**) allowed the calculation of the T2* value within the lesion at $T2^*_{\text{lesion}} = 29.7 \pm 3.0 \text{ ms}$ (n = 5) and in the contralateral cortex, at $T2^*_{\text{cortex}} = 39.4 \pm 1.8 \text{ ms}$ (n = 5) (p < 0.05). T2* evolution over time after injection with BP-IELLQAR-coated nanoparticles is shown in **Figure 3b**.

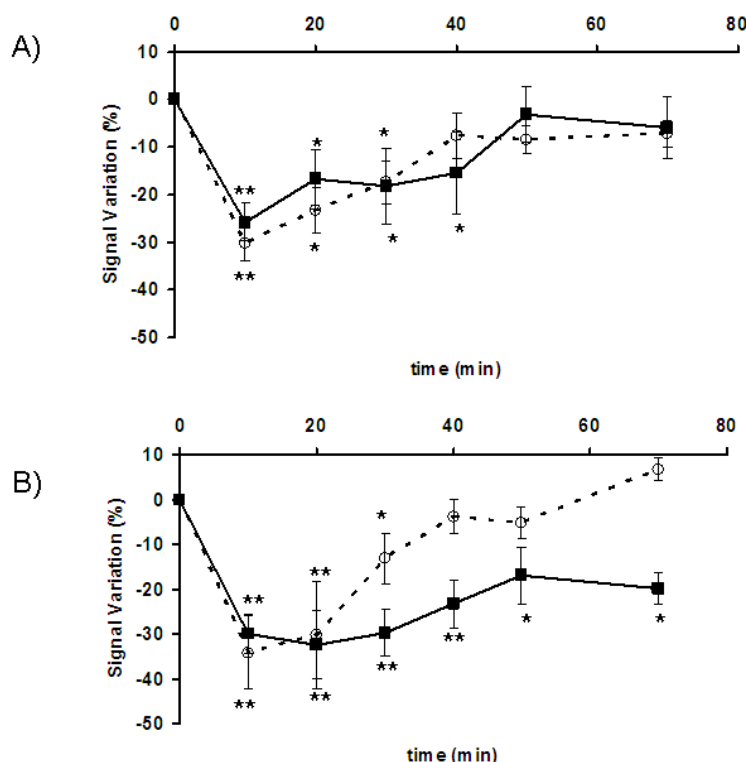


Figure 3: Quantitative assessment of T2* change in traumatized (■; plain line) and contralateral hemisphere (□; dashed line) after injection of non vectorized nanoparticles (A) or BP-IELLQAR vectorized nanoparticles (B). * p < 0.05 and ** p < 0.01 compared to initial T2* value of the considered tissue.

At the first time point post BP-IELLQAR coated nanoparticles injection, a significant 30% reduction in T2* values, both in the lesion ($p = 0.0001$) and the contralateral cortex ($p = 0.0011$) was observed. The T2* value smoothly recovered the pre-injection value after an additional 30 minutes in the non-traumatized cortex but remained under its initial value during the same period of time in the traumatized brain. Indeed, at the 70min. time point, signal intensity is still significantly reduced (-20%) compared to the pre-injection values ($p = 0.013$) (table 1).

Time (min)	Time course of signal reduction after BP-EG3		Time course of signal reduction after BP-IELLQAR	
	Contralateral cortex	Traumatized cortex	Contralateral cortex	Traumatized cortex
10	$-30.3 \pm 3.5^{**}$	$-25.8 \pm 3.9^{**}$	$-34.2 \pm 8.3^{**}$	$-30.1 \pm 4.2^{**}$
20	$-23.3 \pm 4.7^*$	$-16.7 \pm 6.2^*$	$-30.1 \pm 10.1^{**}$	$-32.4 \pm 7.6^{**}$
30	$-17.4 \pm 4.6^*$	$-18.3 \pm 8.0^*$	$-13.1 \pm 5.6^*$	$-29.7 \pm 5.3^{**}$
40	-7.7 ± 4.8	$-15.4 \pm 8.8^*$	-3.8 ± 4.0	$-23.4 \pm 5.2^{**}$
50	5.9 ± 3.0	-3.1 ± 6.0	-5.2 ± 3.5	$-17.0 \pm 6.4^*$
70	-7.2 ± 2.8	-5.9 ± 6.6	6.7 ± 2.5	$-19.9 \pm 3.6^*$

Table 1: Variation with time of the T2* of traumatized or contralateral non-traumatized rat cortex after injection of targeted (BP-IELLQAR) or non-targeted (BP-EG3) contrast agents expressed as the percentage of T2* value prior any injection. * $p < 0.05$ and ** $p < 0.01$ compared to initial T2* value of the considered tissue.

Discussion

The binding of E-selectin to its ligand expressed on the surface of circulating neutrophils is known to initiate rolling, an early step in the recruitment of these cells to a site of injury or inflammation[42, 43]. Starting from this point, numerous biomolecules are produced to interfere with this recruitment[14, 31, 44]. Among the peptides produced, the shortest sequence tested and proven efficient to interact with selectin binding sites, with an $IC_{50} \approx 10 \mu M$, was IELLQAR[31]. Moreover, *in vivo*, this sequence has been shown to significantly reduce the metastatic capability of B16-FTIIIz melanoma cells that constitutively produced sialyl Lewis X [45].

As the present study aimed at the mapping of E-selectin expression *in vivo* using MR enhanced imaging using a specifically designed SPIO targeted contrast agent, we first had to test that the grafting of a bisphosphonate-bearing molecule on the peptide did not impact its binding properties in an animal model of brain injury in which over-expression of this protein has been described [46]. Indeed, this chemical modification was necessary for the stabilization of the iron core in physiological conditions[34, 35]. Another advantage of this grafting was that ^{99m}Tc can be linked to the peptide by chelation via the bisphosphonate group [47] and therefore offers a fast and efficient opportunity to test the modified peptide binding capabilities *in vivo* using γ -counting. Thus, the injection of ^{99m}Tc BP-IELLQAR into rats that have experienced traumatic brain injury induced a significant accumulation of the peptide in the traumatized hemisphere (**Figure 1**) suggesting that the chemical modification of the peptide did not dramatically impact its targeting capabilities. Indeed, the 2-fold increase in activity observed as soon as 1 hour post-trauma, corresponds to specific binding since the leakage of the small radioactive peptide within the interstitial space can be excluded, as in this model, the Blood Brain Barrier is not disrupted at that time[48, 49]. On the contrary, the increase in activity observed at 72h may be attributed at least in part to the Blood Brain Barrier disruption that was shown to take place at that phase of development of the brain trauma [48]. With respect to the fact that ^{99m}Tc BP-IELLQAR accumulated within the traumatized brain, planar scintigraphy imaging was attempted in some rats. However, due to the low activity measured in the brain, ca. 200-300cpm/mg fresh tissues, no images were produced. Moreover, according to the ratio ^{99m}Tc colloid/peptide, it could be calculated that only about 1 over 10^7 molecules of peptide were labelled which could mean that most of the selectin binding sites were targeted by non-radioactive BP-IELLQAR.

Nevertheless, imaging selectin binding sites *in vivo* could be attempted, with a better resolution, using MR imaging since BP-IELLQAR can be used to stabilize iron oxide cores to

produce superparamagnetic nanoparticles, as other bisphosphonates do [34, 35]. Prior to the *in vivo* testing of the nanoparticles, their physical characterization was performed. First of all, targeted nanoparticles were larger than the non-targeted ones and the difference in hydrodynamic diameter could be explained by the length of the peptide grafted on the iron core compared to the length of the BP-EG3. Secondly, despite a slight global difference in zeta potential, the charge distribution and the accessibility of the salt ions were identical for both nanoparticles. Therefore, and except for the size difference, both particles may be considered as equivalent in terms of their physical properties; therefore *in vivo* and behavioural differences may not be attributed to differences in electro-physical properties. As shown in **Figure 2**, the efficient targeting of selectin was achieved with nanoparticles coated with a mixture of only 10% BP-IELLQAR and 90% BP-EG3. The use of 3DmGE sequence with a temporal resolution of ca. 10 min., allowed a dynamic follow up of contrast agent behaviour after injection (**Figure 3**). Thus, the injection of BP-IELLQAR-coated nanoparticles induced a susceptibility effect that, at the early time point, could correspond to tissue perfusion, and was observed in both normal and traumatized brains. Afterwards, a complete clearance of the contrast agent was observed within the contralateral brain whereas the traumatized brain still retained the contrast.

Nevertheless, with respect to this persistent signal reduction in the traumatized brain after BP-IELLQAR injection, two potential limitations need to be highlighted, i.e. the non-specific accumulation of SPIO and the haemorrhagic nature of the lesion and its evolution that may contribute to signal reduction. Indeed, brain trauma induces[7-10] an inflammatory response and, as observed in some inflammatory pathologies such as arthritis or infection [50, 51] a non specific accumulation of SPIO may occur. Even though no direct proof may be given that such a phenomenon did not occur in the study using the targeted SPIO, the lack of long-lasting signal reduction in the group using non-targeted SPIO does not tend to sustain this

hypothesis. Similarly, the signal reduction is probably not due to the worsening of the haemorrhagic status of the lesion, since the reduction is only observed in the lesion of the BP-IELLQAR injected group.

Conclusion:

IELLQAR, a peptide that targets selectin binding site *in vivo* and *in vitro* [31] preserved its binding properties when grafted on SPIO nanoparticles. The synthesized contrast agent can be used to map non-invasively the selectin expression in a traumatic brain injury model. If the nanoparticles are endocytosed in this model in the same way as FITC-E-selectin targeting nanoparticles were endocytosed in an *in vitro* tumor model[21], it may be possible to modify the core of the object or the object itself to deliver relevant therapeutics[52].

Acknowledgements

We would like to thank the technicians from l'animalerie Hospitalo-Universitaire d'Angers for the housing and care of the animals used in this study, Ms. Joëlle Dorat for the synthesis of the nanoparticles and Dr. David Rees for editing the manuscript. This work was partly funded by a grant from la Fondation des Gueules Cassées, Paris, France.

References

1. Thurman D, Alverson C, Dunn K, Guerrero J, JE S (1999) Traumatic brain injury in the United States: a public health perspective. *J Head Trauma Rehabil*, 14:602-615.
2. Kay A, Teasdale G (2001) Head injury in the United Kingdom. *World J Surg*, 25:1210-1220.
3. Mathe J, Richard I, Rome J (2005) Serious brain injury and public health, epidemiologic and financial considerations, comprehensive management and care. *Ann Fr Anesth Reanim*, 24:688-694.
4. Klatzo I (1987) Pathophysiological aspects of brain edema. *Acta Neuropathol (Berl)*, 72:236-239.
5. Kawamata T, Katayama Y, Hovda D, Yoshino A, Becker D (1995) Lactate accumulation following concussive brain injury: the role of ionic fluxes induced by excitatory amino acids. *Brain Research*, 674:196-204.
6. Reinert M, Khaldi A, Zauner A, Doppenberg E, Choi S, Bullock R (2000) High level of extracellular potassium and its correlates after severe head injury: relationship to high intracranial pressure. *J Neurosurg*, 93:800-807.
7. Stanimirovic D, Satoh K (2000) Inflammatory mediators of cerebral endothelium: a role in ischemic brain inflammation. *Brain Pathol*, 10:113-126.
8. Frijns C, Kappelle L (2002) Inflammatory cell adhesion molecules in ischemic cerebrovascular disease. *Stroke*, 33:2115-2122.
9. Danton G, Dietrich W (2003) Inflammatory mechanisms after ischemia and stroke. *J Neuropathol Exp Neurol*, 62:127-136.
10. Williams A, Wei H, Dave J, Tortella F (2007) Acute and delayed neuroinflammatory response following experimental penetrating ballistic brain injury in the rat. *J Neuroinflammation*, 4:17.
11. Wang Q, Tang X, Yenari M (2007) The inflammatory response in stroke. *J Neuroimmunol*, 184:53-68.
12. McEver R (1997) Selectin – carbohydrate interactions during inflammation and metastasis. *Glycoconj J*, 14:585-591.
13. Stoolman L (1989) Adhesion molecules controlling lymphocyte migration. *Cell*, 56:907-910.

14. Phillips M, Nudelman E, Gaeta F, Perez M, Singhal A, Hakomori S, Paulson J (1990) ELAM-1 mediates cell adhesion by recognition of a carbohydrate ligand, sialyl-Lex. *Science*, 250:1130-1132.
15. Ley K (2003) Sulfated sugars for rolling lymphocytes. *J Exp Med*, 198:1285-1288.
16. Kneuer C, Ehrhardt C, Radomski M, Bakowsky U (2006) Selectins--potential pharmacological targets? *Drug Discov Today*, 11:1034-1040.
17. Kang H, Josephson L, Petrovsky A, Weissleder R, Bogdanov AJ (2002) Magnetic resonance imaging of inducible E-selectin expression in human endothelial cell culture. *Bioconjug Chem*, 13:122-127.
18. Sibson N, Blamire A, Bernades-Silva M, Laurent S, Boutry S, Muller R, Styles P, Anthony D (2004) MRI detection of early endothelial activation in brain inflammation. *Magn Reson Med*, 51:248-252.
19. Barber P, Foniok T, Kirk D, Buchan A, Laurent S, Boutry S, Muller R, Hoyte L, Tomanek B, Tuor U (2004) MR molecular imaging of early endothelial activation in focal ischemia. *Ann Neurol*, 56:116-120.
20. Boutry S, Burtea C, Laurent S, Toubreau G, Vander Elst L, Muller R (2005) Magnetic resonance imaging of inflammation with a specific selectin-targeted contrast agent. *Magn Reson Med*, 53:800-807.
21. Funovics M, Montet X, Reynolds F, Weissleder R, Josephson L (2005) Nanoparticles for the optical imaging of tumor E-selectin. *Neoplasia*, 7:892-899.
22. Reynolds P, Larkman D, Haskard D, Hajnal J, Kennea N, George A, Edwards A (2006) Detection of vascular expression of E-selectin in vivo with MR imaging. *Radiology*, 241:469-476.
23. Canet-Soulas E, Letourneur D (2007) Biomarkers of atherosclerosis and the potential of MRI for the diagnosis of vulnerable plaque. *Mag reson mater phys*, 20:129-142.
24. Chapman P, Jamar F, Harrison A, Binns R, Peters A, Haskard D (1994) Noninvasive imaging of E-selectin expression by activated endothelium in urate crystal-induced arthritis. *Arthritis Rheum*, 37:1752-1756.
25. Zinn K, Chaudhuri T, Smyth C, Wu Q, Liu H, Fleck M, Mountz J, Mountz J (1999) Specific targeting of activated endothelium in rat adjuvant arthritis with a 99mTc-radiolabeled E-selectin-binding peptide. *Arthritis Rheum*, 42:641-649.
26. Runnels J, Zamiri P, Spencer J, Veilleux I, Wei X, Bogdanov A, Lin C (2006) Imaging molecular expression on vascular endothelial cells by in vivo immunofluorescence microscopy. *Mol Imaging*, 5:31-40.
27. Lindner J, Song J, Christiansen J, Klivanov A, Xu F, Ley K (2001) Sound assessment of inflammation and renal tissue injury with microbubbles targeted to P-selectin. *Circulation*, 104:2107-2112.

28. Weller G, Villanueva F, Tom E, Wagner W (2003) Targeted ultrasound contrast agents: in vitro assessment of endothelial dysfunction and multi-targeting to ICAM-1 and sialyl Lewisx. *Biotechnol Bioeng*, 92:780-788.
29. Ham A, Goetz D, Klibanov A, Lawrence M (2007) Microparticle adhesive dynamics and rolling mediated by selectin-specific antibodies under flow. *Biotechnol Bioeng*, 96:596-607.
30. Laurent S, Vander Elst L, Fu Y, Muller R (2004) Synthesis and physicochemical characterization of Gd-DTPA-B(sLex)A, a new MRI contrast agent targeted to inflammation. *Bioconj Chem*, 15:99-103.
31. Fukuda M, Ohyama C, Lowitz K, Matsuo O, Pasqualini R, Ruoslahti E, Fukuda M (2000) A peptide mimic of E-selectin ligand inhibits sialyl Lewis X-dependent lung colonization of tumor cells. *Cancer Res*, 60:450-456.
32. Renkonen R, Fukada MN, Petrov L, Paavonen T, Renkonen J, Häyry P, Fukuda M (2002) A peptide mimic of selectin ligands abolishes in vivo inflammation but has no effect on the rat heart allograft survival. *Transplantation*, 74:2-6.
33. Babes L, Denizot B, Tanguy G, Le Jeune J, Jallet P (1999) Synthesis of Iron Oxide Nanoparticles Used as MRI Contrast Agents: A Parametric Study. *J Colloid Interface Sci*, 212:474-482.
34. Portet D, Denizot B, Rump E, Lejeune J-J, P J (2001) Nonpolymeric Coatings of Iron Oxide Colloids for Biological Use as Magnetic Resonance Imaging Contrast Agents. *J Colloid Interface Sci*, 238:37-42.
35. Mowat P, Franconi F, Chapon C, Lemaire L, Dorat J, Hindre F, Benoit JP, Richomme P, Le Jeune JJ (2007) Evaluating SPIO-labelled cell MR efficiency by three-dimensional quantitative T2* MRI. *NMR Biomed*, 20:21-27.
36. Ohshima H (2000) On the General Expression for the Electrophoretic Mobility of a Soft Particle. *J Colloid Interface Sci*, 228:190-193.
37. Vonarbourg A, Saulnier P, Passirani C, Benoit JP (2005) Electrokinetic properties of noncharged lipid nanocapsules: influence of the dipolar distribution at the interface. *Electrophoresis*, 26:2066-2075.
38. Stejskal E, Tanner J (1965) Spin diffusion measurements: spin-echoes in the presence of a time-dependent field gradient. *J Chem Phys*, 42:288-292.
39. Van Putten H, Bouwhuis M, Muizelaar J, Lyeth B, Berman R (2005) Diffusion-weighted imaging of edema following traumatic brain injury in rats: effects of secondary hypoxia. *J Neurotrauma*, 22:857-872.
40. Lythgoe M, Busza A, Calamante F, Sotak C, King M, Bingham A, Williams S, Gadian D (1997) Effects of diffusion anisotropy on lesion delineation in a rat model of cerebral ischemia. *Magn Reson Med*, 38:662-668.

41. Franconi F, Mowat P, Lemaire L, Richomme P, Le Jeune JJ (2006) Single-scan quantitative T2* methods with susceptibility artifact reduction. *NMR Biomed*, 19:527-534.
42. Springer TA (1990) Adhesion receptors of the immune system. *Nature*, 346:425-434.
43. Lasky LA (1995) Selectin-carbohydrate interactions and the initiation of the inflammatory response. *Annu Rev Biochem*, 64:113-139.
44. Martens CL, Cwirla SE, Lee RY, Whitehorn E, Chen EY, Bakker A, Martin EL, Wagstrom C, Gopalan P, Smith CW, et al. (1995) Peptides which bind to E-selectin and block neutrophil adhesion. *J Biol Chem*, 270:21129-21136.
45. Ohyama C, Tsuboi S, Fukuda M (1999) Dual roles of sialyl Lewis X oligosaccharides in tumor metastasis and rejection by natural killer cells. *Embo J*, 18:1516-1525.
46. Raghavendra Rao VL, Dhodda VK, Song G, Bowen KK, Dempsey RJ (2003) Traumatic brain injury-induced acute gene expression changes in rat cerebral cortex identified by GeneChip analysis. *J Neurosci Res*, 71:208-219.
47. McAfee JG, Krauss DJ, Subramanian G, Thomas FD, Roskopf M, Ritter C, Lyons B, Schoonmaker JE, Finn RD (1983) Comparison of 99mTc phosphate and diphosphonate complexes in experimental renal infarcts. *Invest Radiol*, 18:479-484.
48. Pasco A, Lemaire L, Franconi F, Lefur Y, Noury F, Saint-Andre JP, Benoit JP, Cozzone PJ, Le Jeune JJ (2007) Perfusional deficit and the dynamics of cerebral edemas in experimental traumatic brain injury using perfusion and diffusion-weighted magnetic resonance imaging. *J Neurotrauma*, 24:1321-1330.
49. Beaumont A, Fatouros P, Gennarelli T, Corwin F, Marmarou A (2006) Bolus tracer delivery measured by MRI confirms edema without blood-brain barrier permeability in diffuse traumatic brain injury. *Acta Neurochir Suppl*, 96:171-174.
50. Dardzinski BJ, Schmithorst VJ, Holland SK, Boivin GP, Imagawa T, Watanabe S, Lewis JM, Hirsch R (2001) MR imaging of murine arthritis using ultrasmall superparamagnetic iron oxide particles. *Magn Reson Imaging*, 19:1209-1216.
51. Gellissen J, Axmann C, Prescher A, Bohndorf K, Lodemann KP (1999) Extra- and intracellular accumulation of ultrasmall superparamagnetic iron oxides (USPIO) in experimentally induced abscesses of the peripheral soft tissues and their effects on magnetic resonance imaging. *Magn Reson Imaging*, 17:557-567.
52. Beduneau A, Hindre F, Clavreul A, Leroux JC, Saulnier P, Benoit JP (2008) Brain targeting using novel lipid nanovectors. *J Control Release*, 126:44-49.

Legends

Figure 1: Comparison of selectin expression in sham and traumatized rat brains as a function of time using γ -counting after injection of ^{99m}Tc BP-IELLQAR.

* $p < 0.05$ compared to untraumatized brains.

$p < 0.05$ compared to contralateral brain at the same time point. The black boxes correspond to the traumatized hemisphere, the white boxes to contralateral hemisphere.

Figure 2: Typical ADC maps of rat brains about 1h after traumatic brain injury (A & B). Frame C presents the $T2^*$ map corresponding to frame A prior to BP-EG3 (non-targeted nanoparticles) and frame E 70 min after injection. Frame D presents the $T2^*$ maps corresponding to frame B prior to BP-IELLQAR (targeted nanoparticles) and frame F, 70 min after injection.

Figure 3: Quantitative assessment of $T2^*$ change in traumatized (■; plain line) and contralateral hemisphere (□; dashed line) after injection of non vectorized nanoparticles (A) or BP-IELLQAR vectorized nanoparticles (B). * $p < 0.05$ and ** $p < 0.01$ compared to initial $T2^*$ value of the considered tissue.

Table 1: Variation with time of the $T2^*$ of traumatized or contralateral non-traumatized rat cortex after injection of targeted (BP-IELLQAR) or non-targeted (BP-EG3) contrast agents expressed as the percentage of $T2^*$ value prior any injection. * $p < 0.05$ and ** $p < 0.01$ compared to initial $T2^*$ value of the considered tissue.